Ocean turbulent heat flux responses to sea surface salinity variability during Benguela Niños and Niñas

Aroucha, L. C. ORCID: https://orcid.org/0000-0003-1279-1092, Hummels, R. ORCID: https://orcid.org/0000-0002-3746-6213 and Lübbecke, J. F. (2025) Ocean turbulent heat flux responses to sea surface salinity variability during Benguela Niños and Niñas. Geophysical Research Letters, 52 (21). e2025GL117793. ISSN 1944-8007 doi: 10.1029/2025gl117793 Available at https://centaur.reading.ac.uk/127364/

AGU ADVANCING EARTH AND SPACE SCIENCES

Geophysical Research Letters

RESEARCH LETTER
10.1029/2025GL117793

Ocean Turbulent Heat Flux Responses to Sea Surface Salinity Variability During Benguela Niños and Niñas

L. C. Aroucha[1,2], **R. Hummels**[1], **and J. F. Lübbecke**[1,3]

[1]GEOMAR Helmholtz Centre for Ocean Research Kiel, Kiel, Germany, [2]Now at Department of Meteorology, National Centre for Atmospheric Science, University of Reading, Reading, UK, [3]Now at University of Bremen, Bremen, Germany

Key Points:

- Anomalous sea surface salinity can amplify Benguela Niño and Ninã events via changes in stratification and in turbulent heat fluxes
- Stratification anomalies led to nearly three times more cooling from turbulent heat fluxes during the 1997 cold event in comparison to the 1995 warm episode
- For constant dissipation rates of turbulent kinetic energy, anomalous salt advection drives 53% of Angola's spring heat flux variability

Supporting Information:

Supporting Information may be found in the online version of this article.

Correspondence to:

L. C. Aroucha,
l.c.aroucha@reading.ac.uk

Citation:

Aroucha, L. C., Hummels, R., & Lübbecke, J. F. (2025). Ocean turbulent heat flux responses to sea surface salinity variability during Benguela Niños and Niñas. *Geophysical Research Letters*, *52*, e2025GL117793. https://doi.org/10.1029/2025GL117793

Received 25 JUN 2025
Accepted 27 OCT 2025

Abstract Benguela Niño and Niña events are episodes of extreme warming and cooling off Angola with impacts on fisheries, ecosystems, and rainfall in southwest Africa. They are typically forced remotely or locally by variations in equatorial or alongshore winds, respectively. We use an extensive in-situ data set to show that sea surface salinity (SSS) changes can also act as a local forcing that amplifies these extreme warm and cold events by altering the water column stratification and consequently the impact of subsurface mixing. The mixed layer turbulent heat loss during an extreme warm episode with unusually low SSS in 1995 is nearly 3× lower than during a cold event with high SSS in 1997. We also demonstrate that interannual turbulent heat flux variability in early boreal spring off Angola is strongly impacted by salt advection fluctuations, and that this turbulent mixing is significant for altering mixed layer temperatures and restoring its salinities.

Plain Language Summary Benguela Niño and Niña events are periods when the ocean off Angola becomes unusually warm or cold. They are often triggered by wind changes at the equator or along the southwestern African coast, affecting fish populations, marine life, and rainfall. Using observational data, we find that changes in ocean salinity also play a key role in locally amplifying these events. When the ocean surface is less salty, the reduced density results in a more strongly stratified surface layer, which reduces the mixing with cold waters from below, and traps heat near the surface, amplifying the warm events. On the other hand, when the surface ocean is saltier, ambient mixing acts on larger gradients, which leads to heat more easily escaping from the surface to deeper layers, making cold events even colder. We show an example of an extreme warm event with low salinity, during which the ocean surface layer lost three times less heat than during a cold event with high salinity. We also show that in early spring, year-to-year changes in surface salinity are an important driver of heat exchange between the ocean surface and subsurface layers. This mixing process significantly impacts ocean surface temperatures and salinities.

1. Introduction

Benguela Niños and Niñas are events of extremely warm and cold sea surface temperatures (SST) in the coastal region off Angola, usually peaking from February to May, governing the SST interannual variability in the region (Florenchie et al., 2003, 2004; Imbol Koungue & Brandt, 2021; Imbol Koungue et al., 2019; Lübbecke et al., 2010; Shannon et al., 1986). These events significantly impact the southeastern tropical Atlantic productivity, fisheries, and ecosystem management (Binet et al., 2001; Boyer & Hampton, 2001; Gammelsrød et al., 1998; Imbol Koungue et al., 2024; Jarre et al., 2015), as well as rainfall regimes and flooding in coastal Africa (Koseki & Imbol Koungue, 2020; Lutz et al., 2015; Rouault et al., 2003). They are mainly remotely forced via the relaxation or strengthening of the equatorial trade winds and the resulting eastward propagation of equatorial Kelvin waves, which then propagate southward as coastally trapped waves (CTWs) when reaching the African continent (e.g., Bachèlery et al., 2020; Lübbecke et al., 2010). However, in the last decades, local forcing (e.g., changes in meridional winds associated with shifts in the South Atlantic Anticyclone) seems to play an increasingly important role in triggering these events (Imbol Koungue et al., 2021; Lübbecke et al., 2019; Prigent et al., 2020; Richter et al., 2010).

More recently, it has been shown that extreme warm events in the region can additionally be boosted by unusually low sea surface salinity (SSS) in the Angola-Benguela area (ABA, 10°S−20°S, 10°E to the coast), which strengthens the water column stratification, generates barrier layers, and likely reduces the surface cooling via turbulent mixing (Aroucha et al., 2024; Lübbecke et al., 2019; McPhaden et al., 2024). The Congo River is the primary source of low salinity anomalies, connecting the Indian Ocean Dipole to Benguela Niño events through

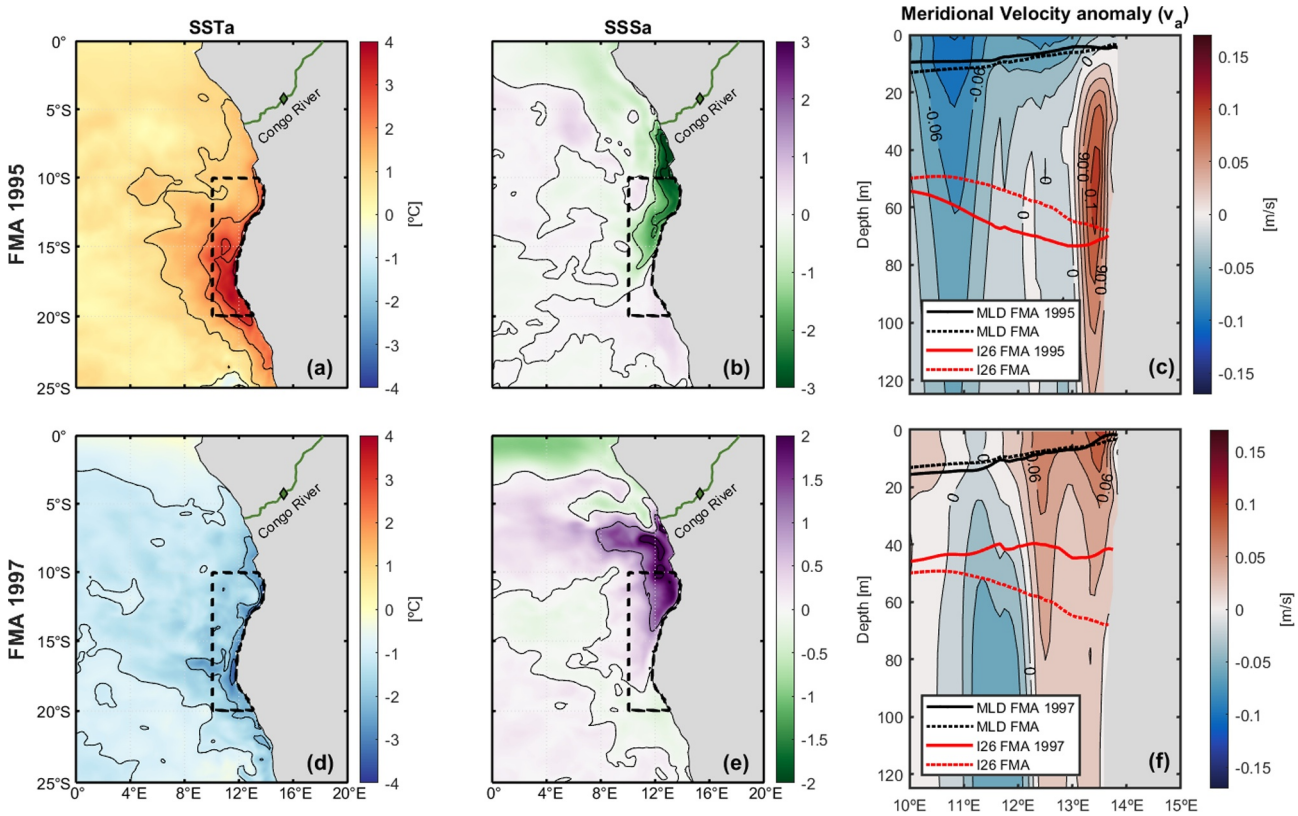

Figure 1. Mean February-March-April (FMA) anomalies of sea surface temperatures (a, d), sea surface salinity (b, e), and ABA-averaged meridional currents, mixed layer depth (black lines), and thermocline depth (I26, red lines) (c, f) from GLORYS12 during 1995 Benguela Niño (a–c) and 1997 Benguela Niña (d–f). The dashed black box indicates the Angola-Benguela area.

increased precipitation over the African continent and subsequent higher river discharge (Jarugula & McPhaden, 2023; McPhaden et al., 2024). Turbulent mixing is indeed of major importance for cooling the SST and for the upward salt flux in this area (Awo et al., 2022; Körner et al., 2023), with the mixing strength depending mainly on the local background stratification (Zeng et al., 2021). Here we aim to quantify for the first time the magnitude of the SSS changes' impact on the turbulent heat fluxes and their subsequent impact on SST within the months of their maximum variability. We further discuss and analyze the hypothesis presented by McPhaden et al. (2024) of enhanced turbulent fluxes cooling the SST during a Benguela Niña event linked to anomalously low freshwater input. For that, we focus on the satellite-era most extreme Benguela Niño and Niña in 1995 and 1997, respectively (Figure 1 and Figure S1 in Supporting Information S1), and also discuss other similar events. By exploring these mechanisms, we attempt to show that the dynamics of freshwater input in the region are of major importance for understanding the local surface temperature variability, and potentially for improving the prediction of Benguela Niño and Niña events, which still poses a challenge (Bachèlery et al., 2025).

2. Data and Methods

2.1. Data Sets

We use an extensive data set of in situ hydrographic measurements from the Nansen Program of the Food and Agriculture Organization of the United Nations, where several research cruises were conducted on board the *R/V Dr. Fridtjof Nansen* (Tchipalanga, Ostrowski, & Dengler, 2018). The cruises occurred twice a year, approximately during austral autumn (February–April, FMA) and austral winter (June-September, JAS; Figure S2 in Supporting Information S1). Here, we use more than 5000 Conductivity-Temperature-Depth (CTD) profiles taken in the ABA (Figure 1) from 1995 to 2014 (Figure S2 in Supporting Information S1).

To estimate the turbulent heat fluxes (J_h) in the ocean, that is, the mixed-layer (ML) turbulent heat loss, we combined CTD profile measurements with ocean turbulence data collected in Angolan waters during seven

research cruises on board of *R/V Meteor* from 2013 to 2022 (Körner et al., 2023b). These measurements were conducted using a free-falling microstructure profiler equipped with two to three airfoil shear sensors from which the dissipation rates of turbulent kinetic energy (TKE, ε) were estimated. For more details, we refer to Hummels et al. (2013, 2014) and Körner et al. (2023, 2024).

Monthly temperature, salinity, and ocean currents were obtained from the Global Ocean Eddy-resolving Reanalysis (GLORYS12, Lellouche et al., 2021), which has a horizontal resolution of 1/12° and 22 levels in the upper 100 m. GLORYS12 is available from 1993 to 2021 and shows good agreement with the in situ temperature and salinity measurements from the Nansen Program (Figure S2 in Supporting Information S1) and the velocity data from a moored acoustic Doppler current profiler off Angola (Aroucha et al., 2024).

Finally, monthly surface rates of evaporation and precipitation, shortwave radiation (SWR), longwave radiation (LWR), latent heat flux (LHF), sensible heat flux (SHF), and 10-m wind components were retrieved from the European Center for Medium-Range Weather Forecasts reanalysis 5 (ERA5, Hersbach et al., 2020). ERA5 has a ¼° resolution, and is available from 1940 onwards. In the present study, we focus on the 20-year measurement period of the Nansen Program, that is, 1995 to 2014.

2.2. Methodology

2.2.1. Definitions

The mixed layer depth (MLD) is defined here as the depth at which the density is increased by 0.125 kg/m^3 compared to the surface value, following Körner et al. (2024). The same criteria was applied to the CTD data and the vertical density profiles derived from GLORYS12 temperature and salinity fields. Thermocline depth is taken as the depth of the 26 kg/m^3 isopycnal, which represents the permanent thermocline depth in the region, that moves vertically with the passage of CTWs (Brandt et al., 2023; Kopte et al., 2017; Tchipalanga, Dengler, et al., 2018).

Following Imbol Koungue et al. (2017, 2019) we characterize an event as a Benguela Niño or Niña when detrended monthly anomalies of ABA-averaged SST exceed ±1 STD for at least three consecutive months. When one of these months additionally features detrended monthly anomalies of ABA-averaged SSS exceeding ±1 STD, the event is also termed "fresh" or "salty." Based on this definition, we find 2 concomitant fresh and warm events (i.e., 1995, 2001) and 3 salty and cold events (i.e., 1997, 2010, 2012) between 1995 and 2014 (Figure S1 in Supporting Information S1).

2.2.2. Turbulent Fluxes Calculation and Error Estimates

Turbulent heat fluxes within the ocean are calculated via the following equation:

$$J_h = -\rho c_p K_\rho \frac{\partial T}{\partial z} \tag{1}$$

where ρ is the seawater density and c_p is the specific heat capacity. $\frac{\partial T}{\partial z}$ is the vertical temperature gradient and K_ρ represents the eddy diffusivity of mass, which is calculated following Osborn (1980): $K_\rho = \Gamma\, \varepsilon\, N^{-2}$. Γ represents the mixing efficiency and is set as 0.2, based on Gregg et al. (2018). From the CTD profiles within the ABA, we calculate the Brunt-Väisäla frequency, N^2, and $\frac{\partial T}{\partial z}$. Vertical measurements in the upper 3 m were discarded. To determine individually each profile's J_h, we converted the vertical coordinate from depth to distance to MLD (i.e., MLD + ΔZ) by binning each profile into a grid with 5 m vertical resolution. Measurements within the ML and 5 m below it were disregarded to avoid ship turbulent effects, and because the mixing efficiency is unknown in weakly stratified waters (Gregg et al., 2018). Measurements were then averaged for each respective depth bin. From the binned profiles of ε and N^2, we estimate K_ρ, followed by the estimation of the J_h also considering the binned profiles of $\frac{\partial T}{\partial z}$. Similarly, turbulent salt fluxes (J_s) were calculated via

$$J_s = K_\rho \frac{\partial S}{\partial z}, \tag{2}$$

where the vertical salinity gradient ($\frac{\partial S}{\partial z}$) was also taken from the CTD profiles, to quantify its importance for the overall SSS change.

From the shear sensor measurements, we estimated ε by using the variance method assuming isotropy, as in Hummels et al. (2013, 2014), and Körner et al. (2023). ε from the 2–3 shear foils were averaged individually for each profile. Even though the microstructure measurements from the research cruises do not overlap temporally with the Nansen Program campaigns, it is still reasonable to assume constant values of ε for the 1995–2014 period, since mixing in this region is driven mostly by internal tides and the tidal energy available is nearly constant throughout the year (Körner et al., 2023; Zeng et al., 2021). Indeed, from the analyzed microstructure measurements, we find that TKE rates are rather similar in the region, and are not influenced by seasonal changes in stratification (Figure S3 in Supporting Information S1). The mean ε is thus assumed to be only a function of bathymetry (Körner et al., 2023, Figure S4 in Supporting Information S1). Hence, we separated both microstructure and CTD profiles in three subregions, following Körner et al. (2023): shallow waters (i.e., depth <75 m); shelf break (i.e., 175 m ≥ depth ≥ 75 m); deep waters (depth >175 m; Figure S4 in Supporting Information S1). After estimating J_h and J_s individually for each profile, we calculated a weighted mean for the ABA, considering that shallow waters cover 4% of the region, while shelf break and deep waters represent 7% and 89%, respectively.

Finally, to compensate for the uneven number of CTD profiles taken in each season (i.e., FMA, JAS), we initially calculated the anomaly for each profile by subtracting the monthly climatological mean. Then, we added the seasonal climatology for each profile individually. Finally, we averaged the profiles for each year's season to get a mean seasonal profile for each of the 20 years analyzed.

Errors in J_h and J_s calculations are estimated based on the 95% confidence limits (CL95), following Hummels et al. (2013, 2014). For N^2, $\frac{\partial T}{\partial z}$, and $\frac{\partial S}{\partial z}$ we convert the standard error (SE) to CL95 via $\mathrm{CL95} = \bar{x} \pm 1.96\,SE$, where $\bar{x}$ is the monthly average of the term x. CL95 for K_ρ, J_h, and J_s are derived via Gaussian error propagation. Finally, for ε, CL95 is obtained via boostrapping.

2.2.3. Mixed Layer Heat and Salt Budgets

To relate the changes in SST and SSS to changes in turbulent heat fluxes, we performed both an ML heat and salt budget analysis. For the ML heat budget, we used

$$\rho\, c_p\, h \frac{\partial T}{\partial t} = -\rho\, c_p\, h\, \boldsymbol{v}\,.\nabla T + q_{\mathrm{net}} + \mathrm{res}_H \tag{3}$$

where T (in °C) and $\boldsymbol{v}$ (in m/s) are the ML temperature and horizontal currents, respectively, and h (in meters) is the MLD. ρ represents the seawater density, and c_p is specific heat capacity. q_{net} (in W/m^2) is the sum of LWR, SHF, LHF and SWR absorbed within the ML, defined by considering an albedo rate of 6% as in Aroucha et al. (2024) and Foltz et al. (2020). res_H is the heat budget residual, which includes the turbulent heat fluxes, vertical temperature covariance and advection, data uncertainty, and processes in temporal and spatial scales smaller than the data set scales here used. Each term represents, from left to right: temperature tendency, horizontal advection, net surface heat flux, and residual.

For the ML salt balance, we consider the following:

$$\frac{\partial S}{\partial t} = -\boldsymbol{v}\,.\nabla S + \frac{S}{h}(E - P) + \mathrm{res}_S \tag{4}$$

where S (in psu) is the ML salinity (MLS), P and E are the precipitation and evaporation rates (m day^{-1}), respectively. res_S is the salt budget residual, which includes vertical advection, salinity covariance, turbulent salinity flux, data uncertainty, and computational errors. Each term represents, from left to right: salt tendency, horizontal advection, local freshwater forcing, and residual. Both heat and salt budgets were estimated for every grid point and then averaged for the ABA. J_h and J_s are not included in the calculation of res_H and res_S, respectively.

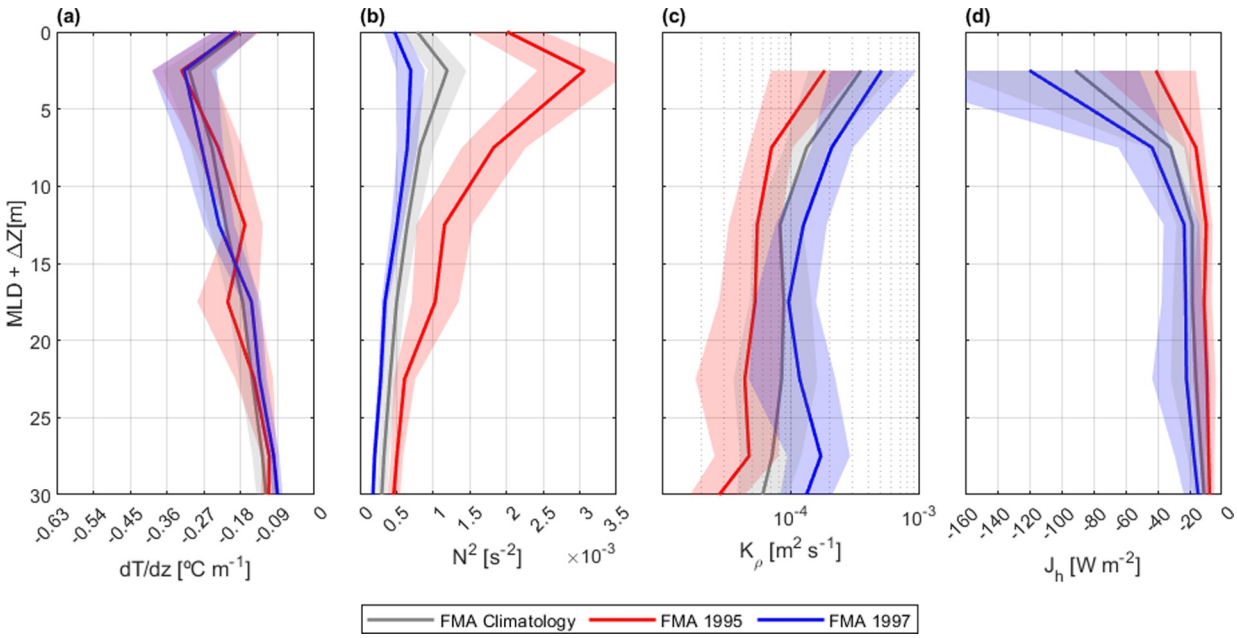

Figure 2. Averaged profiles of the turbulent heat flux terms from *in-situ* profiles. (a) Vertical temperature gradient (°C/m). (b) Squared Brunt-Väisäla frequency (s^{-2}). (c) Eddy diffusivity (m^2/s). (d) Turbulent heat flux (W/m^2). Gray, red, and blue lines indicate FMA climatological, 1995, and 1997 means, respectively. Shaded areas represent 95% confidence level.

3. The Contrasting 1995 and 1997 Extreme Events

The 1995 (1997) Benguela Niño (Niña) events have been extensively documented and discussed in the literature (e.g., Aroucha et al., 2024; Bachèlery et al., 2020; Florenchie et al., 2003, 2004; Gammelsrød et al., 1998; Imbol Koungue et al., 2019; Imbol Koungue & Brandt, 2021; McPhaden et al., 2024). They were predominantly remotely triggered via a relaxation (strengthening) of the equatorial trade winds and the subsequent propagation of equatorial Kelvin waves and CTWs. Local meridional wind fluctuations also likely played a role by contributing to coastal current changes and meridional heat advection (e.g., Aroucha et al., 2024; Richter et al., 2010). The events reached their peak in March (April) with an ABA-averaged FMA mean of +2.5°C (−2.0°C; Figures 1a, 1d and Figure S1a in Supporting Information S1).

Noteworthy, these events oppose each other in terms of SSS (Figures 1b and 1e) and coastal meridional current anomalies at the surface (Figures 1c and 1f). During the 1995 (1997) Benguela Niño (Niña), a plume of negative (positive) SSS anomalies is present in the region with an ABA-averaged FMA mean of −0.67 (+0.61). At the same time, there is an anomalous southward (northward) coastal current. The coastal current changes are likely related to CTW propagation (Bachèlery et al., 2016; Kopte et al., 2017) as indicated by the thermocline depth anomalies (Figures 1c and 1f) and shifts in the local wind stress and wind stress curl (Aroucha et al., 2024; Fennel et al., 2012; Junker et al., 2015, Figure S5 in Supporting Information S1). A propagating CTW during FMA combined with an exceptional CRD is necessary for the low-salinity anomalies to spread southward in this region (Martins & Stammer, 2022). Since salt advection is one of the dominant terms in altering the MLS during boreal late-winter and early-spring (Awo et al., 2022), the combined effects of surface current and freshwater input anomalies likely drove the unusual SSS fields in the region throughout these months (see also Section 5). One effect of the opposite SSS anomalies is evident in the MLD (Figures 1c and 1f), with an apparent ML shoaling (deepening) compared to the FMA climatology during FMA 1995 (1997). Therefore, we further examine the impact of these contrasting SSS anomalies on both the stratification and turbulent heat flux during each event.

4. Turbulent Heat Fluxes

Calculated from Equation 1, the mean ABA FMA turbulent heat loss immediately below the ML was approximately three times stronger during the 1997 Benguela Niña in comparison to the 1995 Benguela Niño (−120.0 [−227.5, −51.3] W/m^2 in 1997 vs. −41.2 [−77.2, −16.3] W/m^2 in 1995; Figure 2d). When averaging from 2 to

15 m below the ML, a similar 3-fold factor is observed (−62.3 [−109.5, −32.2] W/m^2 in 1997 vs. −22.3 [−38.6, −11.0] W/m^2 in 1995; Figure S6a in Supporting Information S1). In both years, J_h was also significantly different from the FMA climatology, especially during FMA 1995. This result indicates that the ML cooling efficiency was much stronger (weaker) during the Benguela Niña (Niño) months with anomalously high (low) SSS. These differences in J_h cannot be related to an increased/decreased vertical temperature gradient (Figure 2a), which shows only slight differences between years at 10 m below the ML. This is true also for temperature profiles from GLORYS12. Instead, it reflects the different K_ρ between these years (Figure 2c), explained here exclusively by the strong stratification differences (Figure 2b), as dissipation rates were assumed constant within the respective years. The mean FMA 1997 N^2 profile characterizes a weak water column stability (unusually reduced stratification down to 30 m below the ML), which results in an elevated J_h. The opposite is true for the mean FMA 1995, when the N^2 peaks at 2.5 m below the ML, being three times stronger than the FMA climatology and more than four times in comparison to 1997 (Figure 2b).

Zeng et al. (2021) showed that the cooling strength of the turbulent heat flux in the Angolan upwelling region depends mainly on the background stratification on which the tidal energy acts. Indeed, our results indicate that, when assuming the tidally driven dissipation rates as constant throughout the year, the different water column stratification creates hugely contrasting J_h in 1995 and 1997 (Figure 2). The same effect is also observed in other years of concomitant anomalous SSS and SST. In FMA 2001, during a weaker Benguela Niño event compared to 1995, but also characterized by unusually low SSS in the ABA (Figure S1 in Supporting Information S1), the increased stratification stood out, and resulted in reduced J_h (i.e., the second lowest mixing rate below the ML in the 20-year analyzed; Figures S6 and S7 in Supporting Information S1). On the other hand, in similar Benguela Niña months coinciding with anomalous positive SSS but smaller in amplitude, J_h is also increased due to reduced water column stability, especially in 2010 (Figures S6 and S7 in Supporting Information S1). It seems likely that the main driver of these stratification changes is the varying SSS, as the vertical temperature gradients are similar. However, since the passage of CTWs triggering the episodes of extreme SSTs in the region is also related to a vertical displacement of the thermocline (e.g., Brandt et al., 2023; Figure 1), also impacting the water column stratification, we further investigate what drives the stratification and the consequent turbulent heat flux variability in the ABA.

5. Salt Advection as the Main Driver of Turbulent Heat Flux Variability

The seasonal cycle of J_h off Angola is connected to seasonal variations in stratification, implying that rather constant mixing by internal tides will be more efficient during the weaker stratification season, that is, boreal summer (Körner et al., 2023). Indeed, Figure S6 in Supporting Information S1 shows that J_h averaged from 2 to 15 m below the ML is higher during JAS than FMA, while its variability is more than two times lower (Figure S6 in Supporting Information S1). Since Benguela Niño/Niña events occur mainly from February to April, we here focus on explaining the J_h variability during FMA. These months also feature maximum SSS variability off Angola, linked to the timing of higher freshwater input by the Congo River north of the ABA (Jarugula & McPhaden, 2023; McPhaden et al., 2024) and increased southward advection of low salinity waters, which climatologically reach as far south as 12°S (Awo et al., 2022; Houndegnonto et al., 2021). This southward advection is likely related to a stronger and shallower Angola Current during these months (Kopte et al., 2017; Tchipalanga, Dengler, et al., 2018). At the same time, the passage of CTWs in the region also occurs in boreal spring. Therefore, the two main mechanisms that would influence the stratification variability within these months, and consequently J_h, are: the passage of a CTW (i.e., temperature-related stratification shifts) and/or changes in ABA SSS.

A ML salt budget analysis shows that anomalous salt advection, that is, the second term in Equation 4, is an important driver of MLS interannual variability in the ABA during FMA (Figure S8b in Supporting Information S1). We attempted to disentangle the individual effects of both anomalous horizontal salinity gradients and velocity anomalies on the overall salinity advection variability (Figure S9 in Supporting Information S1). It appears that the advection variability is similarly influenced by both terms. Additionally, vertical salinity flux across the base of the salt-stratified ML is also an important term for interannual ML salinity changes (J_S in Figure S10b of Supporting Information S1), representing ∼58% of the MLS rate of change, and explaining a great part of the calculated res$_S$ FMA variability (r = 0.71, Figure S8b in Supporting Information S1). In fact, during fresh (salty) events, due to stronger (weaker) vertical salinity gradients, the J_s is higher (lower), acting to restore the MLS (Figures S10 and S11 in Supporting Information S1). Still, the anomalous salt advection explains more than

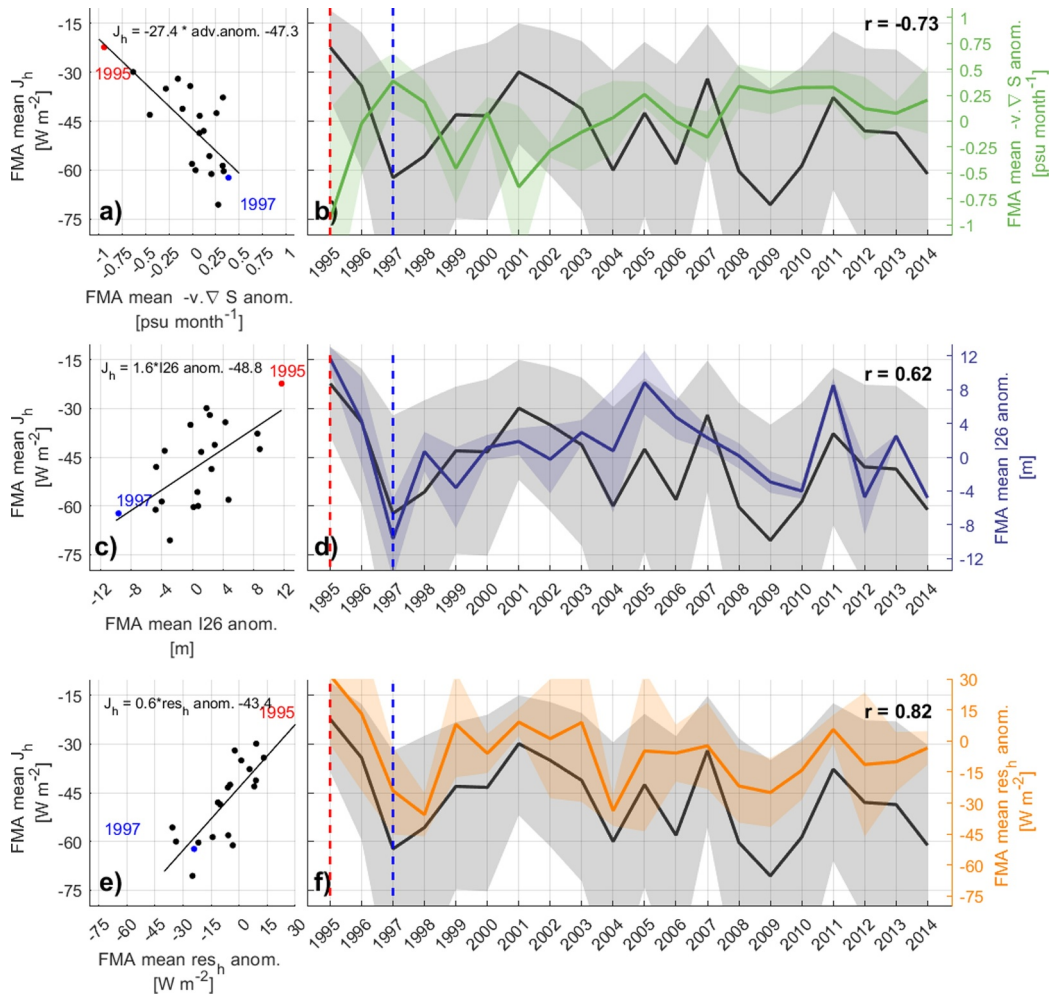

Figure 3. (a, c, e) Scatter diagram and linear regression fit between Angola-Benguela area (ABA) FMA mean J_h averaged from 2 to 15 m below the ML and: ABA FMA mean ML salt advection anomalies (a); ABA FMA mean thermocline depth anomalies (c); ABA FMA mean ML heat budget residual (e). (b, d, f) Time series of ABA FMA mean J_h (black) and: ABA FMA mean ML salt advection anomalies (b); ABA FMA mean thermocline depth anomalies (d); ABA FMA mean ML heat budget residual (f). Red (blue) dots in (a, c, e) and dashed lines in panels (b, d, f) indicate 1995 (1997). Linear least squares regression fit equations are shown in Panels (a, c, and e). Correlation coefficients are shown in Panels (b, d, and f). Shaded areas represent 95% confidence level (for variables on right axis taken from SE). J_h is calculated from in situ profiles, other variables are taken from GLORYS12.

86% of MLS interannual changes (i.e., $r = 0.93$). Hence, we focus on analyzing how the FMA mean J_h correlates with both thermocline and salt advection anomalies.

Anomalies of salt advection are significantly and highly correlated to turbulent heat flux changes in the ABA ($r = -0.73$, p-value <0.05), and explain more than half of the mean FMA J_h variability (53%; Figures 3a and 3b). In fact, the year with the most negative (positive) salt advection anomaly is 1995 (1997). At the same time, thermocline depth anomalies (i.e., temperature-related changes in stratification) also significantly correlate with J_h ($r = 0.62$, p-value <0.05; Figures 3c and 3d), explaining 38% of its FMA variability in the ABA. Both terms impact stratification and consequently the turbulent fluxes, but the role of salt advection is found to prevail. We further performed the same correlation analysis for ABA-averaged FMA mean MLD, Isothermal Layer Depth (ILD), and Barrier Layer Thickness (BLT, i.e. Barrier Layer Thickness = ILD–MLD) anomalies using the Nansen Program CTD profiles. Barrier layers, that is, layers between a salinity dominated mixed layer and a deeper isothermal layer, can indicate an increase in the surface ocean stratification due to changes in SSS and MLD, being mainly present in regions with high freshwater input. Indeed, J_h variability is shown to be more closely related to changes in MLD rather than in ILD (i.e., $r = -0.69$ and -0.41, respectively, not shown), agreeing with a

ML shoaling (deepening) when there is a negative (positive) SSS anomaly, instead of an downward (upward) movement of the thermocline related to the passage of a downwelling (upwelling) CTW. The correlation is even stronger with the BLT anomalies ($r = 0.77$, not shown), with a thicker (thinner) barrier layer here representing stronger (weaker) stratification in the upper ocean layer and consequently less (more) turbulent heat flux, as shown in Aroucha et al. (2024) and McPhaden et al. (2024). Therefore, we can conclude that the anomalous salt advection into ABA is likely the main driver of the FMA stratification variability at the ML base, which results in anomalous J_h off Angola, with the propagating CTWs playing a secondary role in stratification changes.

It has been suggested that turbulent mixing across the base of the ML is an imperative cooling term for SST in this region (Körner et al., 2023). However, its representation in a ML heat budget assessment from observational products is challenging due to its complex calculation, dependent on TKE dissipation rates measurements and eddy diffusivity estimates. Turbulent heat fluxes are then usually represented by the residual term in such budgets (e.g., Aroucha et al., 2024; Imbol Koungue et al., 2024; Körner et al., 2023). Here, by estimating J_h based on in situ CTD profiles and microstructure measurements, we can compare how well the ML heat budget residual (res_H) represents both the magnitude and variability of the turbulent heat fluxes, highlighting the importance of this mixing term for the overall ML temperature changes. Indeed, Figures 3e and 3f show that J_h explains 69% of the res_H interannual variability, which is a crucial term for the ML heat budget (Figure S8a in Supporting Information S1). In terms of magnitude, FMA J_h anomalies represent 82% and 55% of the FMA residual anomaly in 1995 and 1997, respectively (Figure S8a in Supporting Information S1).

6. Summary and Discussion

This study demonstrates the role of SSS anomalies in amplifying Benguela Niño/Niña events by modifying the water column stratification and consequently the efficiency of ocean mixing. It also confirms the hypothesis from McPhaden et al. (2024) that this effect is likewise acting during extreme cold and salty episodes. By quantifying, for the first time, the turbulent heat fluxes during these extreme warm and cold events, we highlight the role of the SSS change forcing mechanism, showing its importance in driving turbulent heat loss variability during boreal spring.

We emphasize that the stratification changes and the subsequent changes in the mixed layer heat loss in the ABA are more strongly associated with ML salt advection anomalies than with the vertical displacement of the thermocline, even though both factors significantly correlate with turbulent heat flux variability (Figures 3a–3d). Coastally trapped wave propagation, however, can also impact the salt advection, since the variability of the Angola current is influenced by these coastal propagating waves (Bachèlery et al., 2016; Tchipalanga, Dengler, et al., 2018). Martins and Stammer (2022) actually suggested the need for a combined propagating CTW with an increased Congo River freshwater discharge for the low-salinity plume to reach far enough south to impact the ABA.

Our findings underline that while freshwater input and associated SSS anomalies in the ABA do not necessarily trigger Benguela Niños and Niñas, they can act as an important local forcing that amplifies these events by altering vertical heat exchange. This study provides a novel quantification of the salinity impact, elucidating the previously overlooked mechanism of the effect of Congo River discharge on SST variability off Angola. This mechanism has gained increased visibility in recent years (Aroucha et al., 2024; Lübbecke et al., 2019; McPhaden et al., 2024), with areas near the Congo River mouth having been pointed out by deep learning models as potential regions of predictability of Benguela Niños, likely associated with SSS changes (Bachèlery et al., 2025). Consequently, monitoring the Congo River basin hydrology and the southeastern Tropical Atlantic SSS variability could significantly improve the representation of these acute events in forecast models (McPhaden et al., 2024). In summary, our work quantitatively affirms the importance of this freshwater-driven mechanism, highlighting the critical role of stratification changes in modulating turbulent heat loss during such extreme events.

Conflict of Interest

The authors declare no conflicts of interest relevant to this study.

Data Availability Statement

The hydrographic data from the Nansen Programme (Tchipalanga, Ostrowski, & Dengler, 2018) and the microstructure data from the research cruises (Körner et al., 2023b) are publicly available from PANGAEA. GLORYS12 product is publicly available from Copernicus Marine Service (Lellouche et al., 2021). Surface heat fluxes and wind data from ERA5 reanalysis are publicly available from ECMWF's Copernicus Climate Data Store (Hersbach et al., 2020).

Acknowledgments
This study was supported by the German Academic Exchange Service (Deutscher Akademischer Austauschdienst) Doctoral Research Grant (57552340). We thank the captains, crews, scientists, and technicians involved in several research cruises in the Angola-Namibian waters. We also thank the two anonymous reviewers for their valuable comments and suggestions. Open Access funding enabled and organized by Projekt DEAL.

References

Aroucha, L. C., Lübbecke, J. F., Körner, M., Imbol Koungue, R. A., & Awo, F. M. (2024). The influence of freshwater input on the evolution of the 1995 Benguela Niño. *Journal of Geophysical Research: Oceans*, *129*(2), e2023JC020241. https://doi.org/10.1029/2023JC020241

Awo, F. M., Rouault, M., Ostrowski, M., Tomety, F. S., Da-Allada, C. Y., & Jouanno, J. (2022). Seasonal cycle of sea surface salinity in the Angola upwelling system. *Journal of Geophysical Research: Oceans*, *127*(7), e2022JC018518. https://doi.org/10.1029/2022JC018518

Bachèlery, M., Illig, S., & Dadou, I. (2016). Interannual variability in the South- East Atlantic Ocean, focusing on the Benguela Upwelling System: Remote versus local forcing. *Journal of Geophysical Research: Oceans*, *121*(1), 284–310. https://doi.org/10.1002/2015JC011168

Bachèlery, M.-L., Brajard, J., Patacchiola, M., Illig, S., & Keenlyside, N. (2025). Predicting Atlantic and Benguela Niño events with deep learning. *Science Advances*, *11*(14), eads5185. https://doi.org/10.1126/sciadv.ads5185

Bachèlery, M.-L., Illig, S., & Rouault, M. (2020). Interannual Coastal trapped waves in the Angola-Benguela upwelling system and Benguela Niño and Niña events. *Journal of Marine Systems*, *203*, 103262. https://doi.org/10.1016/j.jmarsys.2019.103262

Binet, D., Gobert, B., & Maloueki, L. (2001). El Niño-like warm events in the Eastern Atlantic (6°N and 20°S) and fish availability from Congo to Angola (1964–1999). *Aquatic Living Resources*, *14*(2), 99–113. https://doi.org/10.1016/S0990-7440(01)01105-6

Boyer, D. C., & Hampton, I. (2001). An overview of the living marine resources of Namibia. *South African Journal of Marine Science*, *23*(1), 5–35. https://doi.org/10.2989/025776101784528953

Brandt, P., Alory, G., Awo, F. M., Dengler, M., Djakouré, S., Imbol Koungue, R. A., et al. (2023). Physical processes and biological productivity in the upwelling regions of the tropical Atlantic. *Ocean Science*, *19*(3), 581–601. https://doi.org/10.5194/os-19-581-2023

Fennel, W., Junker, T., Schmidt, M., & Mohrholz, V. (2012). Response of the Benguela upwelling systems to spatial variations in the wind stress. *Continental Shelf Research*, *45*, 65–77. https://doi.org/10.1016/j.csr.2012.06.004

Florenchie, P., Lutjeharms, J. R. E., Reason, C. J. C., Masson, S., & Rouault, M. (2003). The source of Benguela Niños in the South Atlantic Ocean. *Geophysical Research Letters*, *30*(10), 2003GL017172. https://doi.org/10.1029/2003GL017172

Florenchie, P., Reason, C. J. C., Lutjeharms, J. R. E., Rouault, M., Roy, C., & Masson, S. (2004). Evolution of interannual warm and cold events in the southeast Atlantic Ocean. *Journal of Climate*, *17*(12), 2318–2334. https://doi.org/10.1175/1520-0442(2004)017<2318:EOIWAC>2.0.CO;2

Foltz, G. R., Hummels, R., Dengler, M., Perez, R. C., & Araujo, M. (2020). Vertical turbulent cooling of the mixed layer in the Atlantic ITCZ and trade wind regions. *Journal of Geophysical Research: Oceans*, *125*(2), e2019JC015529. https://doi.org/10.1029/2019JC015529

Gammelsrød, T., Bartholomae, C. H., Boyer, D. C., Filipe, V. L. L., & O'Toole, M. J. (1998). Intrusion of warm surface water along the Angolan-Namibian coast in February–March 1995: The 1995 Benguela Niño. *South African Journal of Marine Science*, *19*(1), 41–56. https://doi.org/10.2989/025776198784126719

Gregg, M. C., D'Asaro, E. A., Riley, J. J., & Kunze, E. (2018). Mixing efficiency in the ocean. *Annual Review of Marine Science*, *10*(1), 443–473. https://doi.org/10.1146/annurev-marine-121916-063643

Hersbach, H., Bell, B., Berrisford, P., Hirahara, S., Horányi, A., Muñoz-Sabater, J., et al. (2020). The ERA5 global reanalysis. *Quarterly Journal of the Royal Meteorological Society*, *146*(730), 1999–2049. https://doi.org/10.1002/qj.3803

Houndegnonto, O. J., Kolodziejczyk, N., Maes, C., Bourlès, B., Da-Allada, C. Y., & Reul, N. (2021). Seasonal variability of freshwater plumes in the eastern Gulf of Guinea as inferred from satellite measurements. *Journal of Geophysical Research: Oceans*, *126*(5). https://doi.org/10.1029/2020jc017041

Hummels, R., Dengler, M., & Bourlès, B. (2013). Seasonal and regional variability of upper ocean diapycnal heat flux in the Atlantic cold tongue. *Progress in Oceanography*, *111*, 52–74. https://doi.org/10.1016/j.pocean.2012.11.001

Hummels, R., Dengler, M., Brandt, P., & Schlundt, M. (2014). Diapycnal heat flux and mixed layer heat budget within the Atlantic Cold Tongue. *Climate Dynamics*, *43*(11), 3179–3199. https://doi.org/10.1007/s00382-014-2339-6

Imbol Koungue, R. A., & Brandt, P. (2021). Impact of intraseasonal waves on Angolan warm and cold events. *Journal of Geophysical Research: Oceans*, *126*(4), e2020JC017088. https://doi.org/10.1029/2020JC017088

Imbol Koungue, R. A., Brandt, P., Lübbecke, J., Prigent, A., Martins, M. S., & Rodrigues, R. R. (2021). The 2019 Benguela Niño. *Frontiers in Marine Science*, *8*, 800103. https://doi.org/10.3389/fmars.2021.800103

Imbol Koungue, R. A., Brandt, P., Prigent, A., Aroucha, L. C., Lübbecke, J., Imbol Nkwinkwa, A. S. N., et al. (2024). Drivers and impact of the 2021 extreme warm event in the tropical Angolan upwelling system. *Scientific Reports*, *14*(1), 16824. https://doi.org/10.1038/s41598-024-67569-7

Imbol Koungue, R. A., Illig, S., & Rouault, M. (2017). Role of interannual Kelvin wave propagations in the equatorial Atlantic on the Angola Benguela Current system. *Journal of Geophysical Research: Oceans*, *122*(6), 4685–4703. https://doi.org/10.1002/2016JC012463

Imbol Koungue, R. A., Rouault, M., Illig, S., Brandt, P., & Jouanno, J. (2019). Benguela Niños and Benguela Niñas in Forced Ocean Simulation from 1958 to 2015. *Journal of Geophysical Research: Oceans*, *124*(8), 5923–5951. https://doi.org/10.1029/2019JC015013

Jarre, A., Hutchings, L., Kirkman, S. P., Kreiner, A., Tchipalanga, P. C. M., Kainge, P., et al. (2015). Synthesis: Climate effects on biodiversity, abundance and distribution of marine organisms in the Benguela. *Fisheries Oceanography*, *24*(S1), 122–149. https://doi.org/10.1111/fog.12086

Jarugula, S., & McPhaden, M. J. (2023). Indian Ocean Dipole affects eastern tropical Atlantic salinity through Congo River Basin hydrology. *Communications Earth & Environment*, *4*(1), 366. https://doi.org/10.1038/s43247-023-01027-6

Junker, T., Schmidt, M., & Mohrholz, V. (2015). The relation of wind stress curl and meridional transport in the Benguela upwelling system. *Journal of Marine Systems*, *143*, 1–6. https://doi.org/10.1016/j.jmarsys.2014.10.006

Kopte, R., Brandt, P., Dengler, M., Tchipalanga, P. C. M., Macuéria, M., & Ostrowski, M. (2017). The Angola Current: Flow and hydrographic characteristics as observed at 11°S. *Journal of Geophysical Research: Oceans*, *122*(2), 1177–1189. https://doi.org/10.1002/2016JC012374

Körner, M., Brandt, P., & Dengler, M. (2023b). Upper-ocean microstructure data from the tropical Angolan upwelling system [Dataset]. *PANGAEA*. https://doi.org/10.1594/PANGAEA.953869

Körner, M., Brandt, P., & Dengler, M. (2023). Seasonal cycle of sea surface temperature in the tropical Angolan Upwelling System. *Ocean Science*, *19*(1), 121–139. https://doi.org/10.5194/os-19-121-2023

Körner, M., Brandt, P., Illig, S., Dengler, M., Subramaniam, A., Bachèlery, M.-L., & Krahmann, G. (2024). Coastal trapped waves and tidal mixing control primary production in the tropical Angolan upwelling system. *Science Advances*, *10*(4), eadj6686. https://doi.org/10.1126/sciadv.adj6686

Koseki, S., & Imbol Koungue, R. A. (2020). Regional atmospheric response to the Benguela Niñas. *International Journal of Climatology*, *41*(S1). https://doi.org/10.1002/joc.6782

Lellouche, J.-M., Greiner, E., Bourdallé Badie, R., Garric, G., Melet, A., Drévillon, M., et al. (2021). The Copernicus global 1/12 oceanic and sea ice GLORYS12 reanalysis. *Frontiers in Earth Science*, *9*, 1–27. https://doi.org/10.3389/feart.2021.698876

Lübbecke, J. F., Böning, C. W., Keenlyside, N. S., & Xie, S. (2010). On the connection between Benguela and equatorial Atlantic Niños and the role of the South Atlantic Anticyclone. *Journal of Geophysical Research: Oceans*, *115*(C9), 2009JC005964. https://doi.org/10.1029/2009JC005964

Lübbecke, J. F., Brandt, P., Dengler, M., Kopte, R., Lüdke, J., Richter, I., et al. (2019). Causes and evolution of the southeastern tropical Atlantic warm event in early 2016. *Climate Dynamics*, *53*(1–2), 261–274. https://doi.org/10.1007/s00382-018-4582-8

Lutz, K., Jacobeit, J., & Rathmann, J. (2015). Atlantic warm and cold water events and impact on African west coast precipitation. *International Journal of Climatology*, *35*(1), 128–141. https://doi.org/10.1002/joc.3969

Martins, M. S., & Stammer, D. (2022). Interannual variability of the Congo River plume-induced sea surface salinity. *Remote Sensing*, *14*(4), 1013. https://doi.org/10.3390/rs14041013

McPhaden, M. J., Jarugula, S., Aroucha, L. C., & Lübbecke, J. F. (2024). Indian Ocean Dipole intensifies Benguela Niño through Congo River discharge. *Communications Earth & Environment*, *5*(1), 779. https://doi.org/10.1038/s43247-024-01955-x

Osborn, T. R. (1980). Estimates of the local rate of vertical diffusion from dissipation measurements. *Journal of Physical Oceanography*, *10*(1), 83–89. https://doi.org/10.1175/1520-0485(1980)010<0083:EOTLRO>2.0.CO;2

Prigent, A., Imbol Koungue, R. A., Lübbecke, J. F., Brandt, P., & Latif, M. (2020). Origin of weakened interannual sea surface temperature variability in the southeastern tropical Atlantic Ocean. *Geophysical Research Letters*, *47*(20), e2020GL089348. https://doi.org/10.1029/2020GL089348

Richter, I., Behera, S. K., Masumoto, Y., Taguchi, B., Komori, N., & Yamagata, T. (2010). On the triggering of Benguela Niños: Remote equatorial versus local influences. *Geophysical Research Letters*, *37*(20), 2010GL044461. https://doi.org/10.1029/2010GL044461

Rouault, M., Florenchie, P., Fauchereau, N., & Reason, C. J. C. (2003). South East tropical Atlantic warm events and southern African rainfall. *Geophysical Research Letters*, *30*(5), 2002GL014840. https://doi.org/10.1029/2002GL014840

Shannon, L. V., Boyd, A. J., Brundrit, G. B., & Taunton-Clark, J. (1986). On the existence of an El Niño-type phenomenon in the Benguela system. *Journal of Marine Research*, *44*(3), 495–520. https://doi.org/10.1357/002224086788403105

Tchipalanga, P., Dengler, M., Brandt, P., Kopte, R., Macuéria, M., Coelho, P., et al. (2018). Eastern boundary circulation and hydrography off Angola: Building Angolan oceanographic capacities. *Bulletin of the American Meteorological Society*, *99*(8), 1589–1605. https://doi.org/10.1175/BAMS-D-17-0197.1

Tchipalanga, P., Ostrowski, M., & Dengler, M. (2018). Physical oceanography on the Angolan continental shelf and Cabinda [Dataset]. *PANGAEA*. https://doi.org/10.1594/PANGAEA.886492

Zeng, Z., Brandt, P., Lamb, K. G., Greatbatch, R. J., Dengler, M., Claus, M., & Chen, X. (2021). Three-Dimensional numerical simulations of internal tides in the Angolan upwelling Region. *Journal of Geophysical Research: Oceans*, *126*(2), e2020JC016460. https://doi.org/10.1029/2020JC016460